CrossMark

Wind turbine gearbox fault diagnosis based on symmetrical components and frequency domain

Labar Hocine[1] · Zerzouri Nora[1] · Kelaiaia Mounia Samira[1]

Abstract The region of Adrar in Algeria is the windiest in the country; it is for this reason the electricity and gas company "Sonelgaz" has placed a wind farm of about 10 MW. Since it is a Saharan region, the wind is sandy, rich in silica that can damage the teeth of wind gearbox. The present work proposes a method which can make an early diagnosis of the broken tooth and its location in the gearbox, before the general breakdown. The modeling of defaults inside the turbine gearbox by symmetrical components technique is proposed successfully and for the first time in the field of diagnostics (usually this technique is used in the power grid lines short circuits analysis), associated with frequency response analysis. In addition, as it is impossible to install sensors at different parts, the increase in temperature and vibration inside the gearbox due to default, a sensor-less fault diagnosis based on the analysis of power signal generated by the wind turbine is presented and detailed. Furthermore, the peculiarity of this work is the modeling of unbalance forces caused by teeth failure on both the slow shaft and the fast shaft of the gearbox, which has never been considered before. It has been proven that this proposal allows a precise location of the broken tooth and the concerned gear inside the gearbox.

Keywords Wind · Gearbox · Diagnosis · Symmetrical component · Frequency domain · Imbalanced blade forces

✉ Labar Hocine
  hocine.labar@univ-annaba.dz

[1] Laboratoire d'Electrotechnique d'Annaba, Faculty of Engineering Sciences, University of Badji Mokhtar-Annaba, B.P. 12, 23000 Annaba, Algeria

1 Introduction

The wind turbine extracts its energy from the wind and then it is transmitted to the generator through its rotor. We must distinguish between the wind energy P_{wind} (1) and the energy captured by the blades P_g (2) (there are usually three in number). It will be consumed in the form of apparent power load S_L.

$$P_{\text{wind}} = \frac{1}{2}\rho A V_{\text{wind}}^3 \tag{1}$$

$$P_g = C_{\text{p}}\frac{1}{2}\rho A V_{\text{wind}}^3 \tag{2}$$

where, ρ is air density, A is area swept by blades, V_{wind} is wind speed and C_{p} is the power coefficient.

Wind forces exerted on the blades by the radius R produce the primary rotation torque and reach the gearbox.

Gearboxes are problematic by the very nature of the numerous moving parts and subsystems that are required for their operation and the demanding nature of the wind turbine application itself.

However, after many years of wind power production, the statistical investigations show the weakness of gearboxes because of their complexity and multiple moving parts. Because of the high position of the gearbox on the tower, the frequent maintenance is complex, and requires more cost and time.

The general benefits arising from introducing diagnosis can be summed up as follows:

– Avoidance of premature breakdown. Early fault detection allows to prevent catastrophic failures to occur. For example, late detection of a bearing fault may in the worst case simply complete destruction of gearbox.

– Reduction of maintenance costs, by using on-line monitoring inspections can be avoided or inspection intervals increased.
– Supervision and Diagnosis at remote sites. In fact, large wind turbines are usually built at remote sites (as it is the case for Adrar in Algeria) where on-line monitoring systems can detect such changes at an early stage and, if integrated in a network, send a warning and diagnostic details to the maintenance staff.
– Improvement of capacity factor, when a good estimation of the remaining useful life is available, repairs or replacements action can be scheduled during time frames. Capacity factor is defined as the ratio between the actual production over a given period of time and the amount of power the turbine would have produced running at full capacity during the same period of time

A turbine's gearbox is a major contributor of machine noise maintenance. One reason is the tooth mesh of the gear wheels. The structure-borne noise generated by the tooth mesh propagates through the roller bearings to the gearbox and after that to the nacelle, and finally this noise radiates to the environment. Turbine noise is a much more serious issue in community-based wind power applications where turbines are located in the places where people live and work.

Diagnostic techniques defects are very various [1–5], for example the frequency response analysis "FRA", artificial neural network "ANN" and genetic algorithm "GA" etc…The aim of this work is to develop an effective sensorless technique for detecting faults. This is not based on preset manufacturer data (FRA), or after repetitive computation in the case of intelligent technique (ANN, GA . . .). The proposal is very useful for the unreachable part [6,7], as the case for wind turbine where it can be applied to different gearbox types without any comparison to a classified or preset reference signal as it is the case for ANN or GA applications.

Wind farm and especially for the offshore, the online control [8] is of great importance in sustainability. Conventional condition monitoring techniques, such as vibration and generator current signal analysis, require the deployment of a variety of sensors and are computationally intensive analysis techniques. A great number of sensors reduced considerably the reliability of the entire system. Many works use the capability of the monitoring model to detect changes in the gearbox vibration excitement evaluated and compared to the collected data [9]. Because of wind speed variation this method requires a large data memory. The effectiveness of FFT signal processing is also investigated [10]. The major problem of this method is the noise, which can be filtered by the combination of artificial neural network and wavelet methods [11,12]. Once again this can take more computation time. In this work, only the power is measured and analyzed [13]. But the novelty in this paper is the detection of fail-
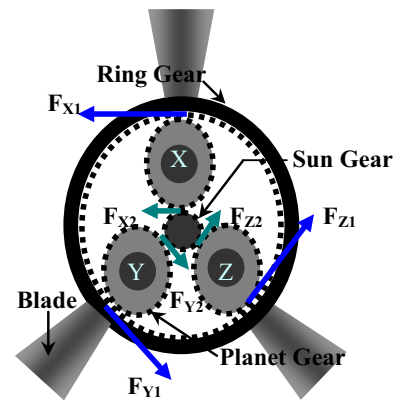

Fig. 1 Wind gearbox structure design

ures both in sun, planet and ring gear, unlike the detection of only the planet gear proposed in [14]. Furthermore, the unbalanced blade torque is modeled.

The wind turbine gearbox is an inaccessible mechanical moving part; in addition, it is immersed in the oil for the lubrication and cooling. The insertion of sensors increases the risk of defects and it can generate additional costs. So we are challenged to develop a technique able to analyze the available parameters which are strongly influenced by this type of defect.

2 Modeling and diagnostic technique

The three wind generator blades generate three identical forces for exact 120° phase shifts. Unbalanced conditions may arise from unequal force or phase shift. However, there are certain situations that can cause unbalanced operations [15]. The most of these would be a teeth loss in the gearbox [4]. Gearboxes are parts of almost every electrical motor. In addition, they are inherently subject to dynamic contact forces with high amplitudes. In the region close to the contact surfaces, the teeth stress is locally very high. Thus, after some time of operation a localized defect growing with time will appear.

Considering the configuration of the gearbox, Fig. 1, when one of these teeth breaks the wind generator does not rotate in free wheel during this time, but it gets weaker torque. The construction of the multiplier allows in the healthy case, balanced forces exerted in time and space Fig. 1. With the loss of a tooth during its passage, the force that would normally exercise becomes zero. Therefore, the wind generator shaft will be subjected to unbalanced forces Fig. 2. This consideration has never been taken into account; it is also the cause of the vibration amplification [16] and in this work it has been modeled and detailed.

Each part of the gearbox has its own signal signature failure, detected thanks to the comparison with data. But the
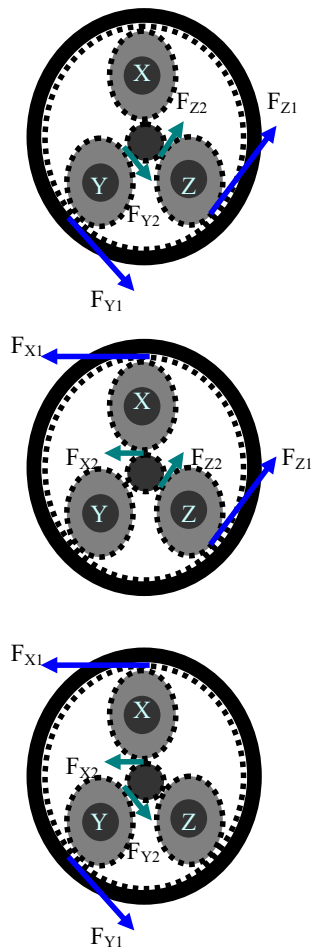
Fig. 2 Crash tooth effect in unbalanced forces

Fig. 3 Symmetrical components redistribution force

analytical development of blade torques can make a relationship between wind speed and fault location in the gearbox. The first part of this work is to make a model of a tooth loss [17,18], which can be as well as at the ring gear, planet gear or sun gear. To do it a symmetrical components technique is proposed allowing fictitious redistribution of balanced forces [19].

3 Symmetrical components systems

The wind generation system operates in a balanced three-blade force. When a gear tooth loss occurs, the system goes from a balanced condition to an unbalanced condition. Because of the difficult modeling of faults at the wind turbine gearboxes, the researchers use an empirical model [19], or a designer database, and never, the effect of this type of faults in the unbalance of forces is considered. By the method of symmetrical components, a set of unbalanced forces may be resolved into systems of balanced force equal in number to the number of planet gear involved.
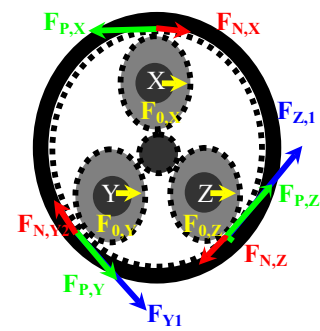
The basis for this analytical technique is a transformation of the three forces into a second set of forces (3). This second set is known as the symmetrical components.

The transformation is defined as:

$$\begin{bmatrix} F_{P,X,1,2} \\ F_{N,X,1,2} \\ F_{0,X,1,2} \end{bmatrix} = \frac{1}{3} \begin{bmatrix} 1 & a & a^2 \\ 1 & a^2 & a \\ 1 & 1 & 1 \end{bmatrix} \begin{bmatrix} F_{X,1,2} \\ F_{Y,1,2} \\ F_{Z,1,2} \end{bmatrix} \tag{3}$$

where the complex number a is: $a = e^{j2\pi/3} = -\frac{1}{2} + j\frac{\sqrt{3}}{2}$, the indexes 1,2 represent the slow and fast shaft, respectively.

The three component variables (force) $F_{P,X}, F_{N,X}, F_{0,X}$ are called, respectively, positive sequence, negative sequence and zero sequence. They are called symmetrical components because, taken separately, they transform into symmetrical sets of forces.

$F_{N,X}$ is called negative sequence force because the sequence of forces is reversed. Note that the negative sequence set is still balanced because the force components still have the same magnitude $\{|F_{P,X}| = F_{P,Y}| = F_{P,Z}|; |F_{N,X}| = F_{N,Y}| = F_{N,Z}|; |F_{0,X}| = F_{0,Y}| = F_{0,Z}|\}$ and are separated by 120°. The only difference between positive and negative sequence is the rotation direction Fig. 3. Consequence of this unbalance leads to the creation of antagonistic couples, and to vibration of the nacelle. With time it will conduct to a misalignment of the gearbox with the generator shaft and leads to failure

If the three forces are equal $\{F_{X,1,2} = F_{Y,1,2} = F_{Z,1,2}\}$ (balanced) the negative and zero sequences are nil, only the positive sequence exists (4), so $F_{P,X,1,2} = F_{X,1,2}$ and the developed turbine's torque takes the value $T_{1,2} = 3F_{X,1,2}R_{1,2}$

$$\begin{bmatrix} F_{P,X,1,2} \\ F_{N,X,1,2} \\ F_{0,X,1,2} \end{bmatrix} = \frac{1}{3} \begin{bmatrix} 3 \\ 0 \\ 0 \end{bmatrix} \begin{bmatrix} F_{X,1,2} \\ F_{Y,1,2} \\ F_{Z,1,2} \end{bmatrix} \tag{4}$$

And in unbalanced case positive, negative and zero sequences exist Fig. 4. The zero sequence $T_{0,1,2}$ does not produce any torque; the negative sequence $T_{N,1,2}$ develops a torque

Fig. 4 Symmetrical
components space vector

Unbalanced blade forces

Positive sequence

Negative sequence
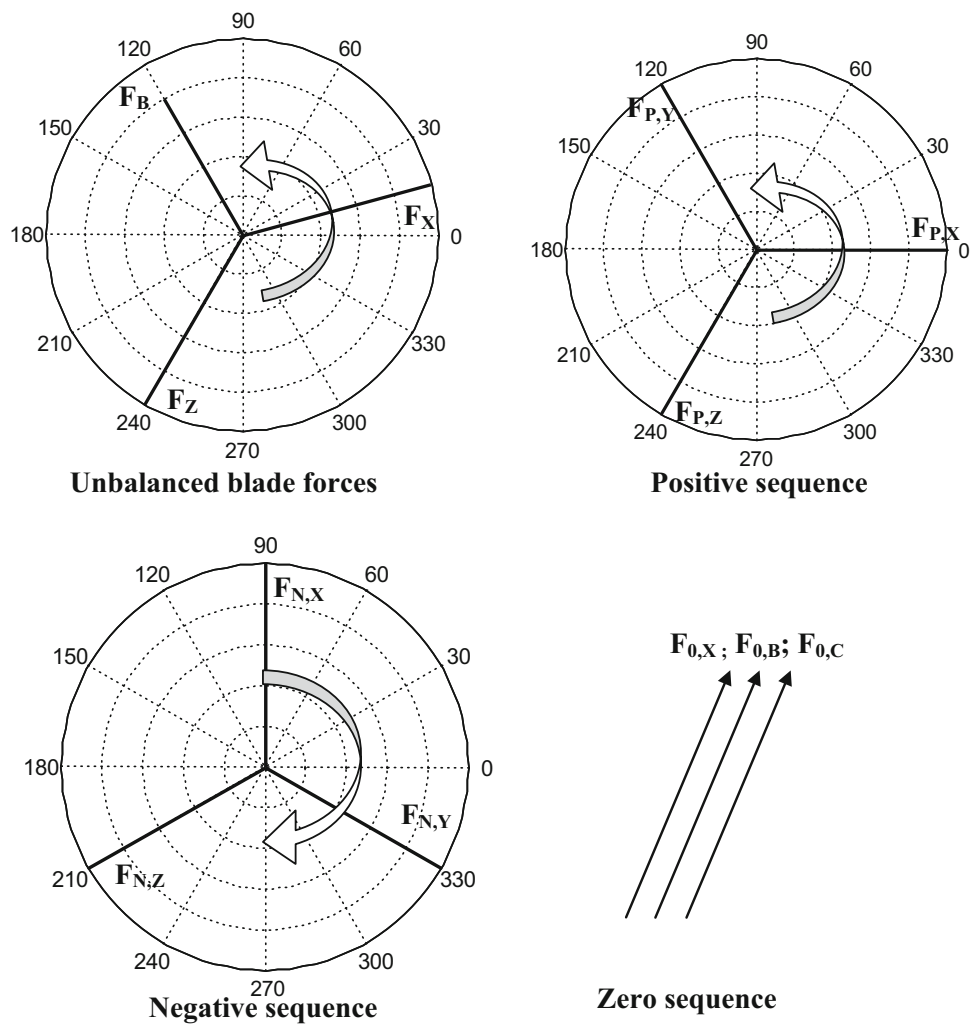
Zero sequence

Table 1 Symmetrical
components forces faults

Force lost	Positive sequence $F_{P,X}$		Negative sequence $F_{N,X}$		Zero sequence $F_{0,X}$	
	Magnitude	Phase shift	Magnitude	Phase shift	Magnitude	Phase shift
0	1	0	0	0	0	0
$F_{X,1}$	2/3	0	$-1/3$	0	$-1/3$	0
$F_{Y,1}$	2/3	0	1/3	60°	1/3	$-60°$
$F_{Z,1}$	2/3	0	1/3	$-60°$	1/3	60°

assumed as a brake torque and the negative sequence $T_{P,1,2}$ is the generator torque. The resultant torque is shown in (5).

$$T_{1,2} = 3T_{P,1,2} - 3T_{N,1,2} \tag{5}$$

Consequently, the produced wind power (6) is reduced, the vibration and noise increase because of the negative sequence

$$S_L = T_{1,2}\omega_{1,2} \tag{6}$$

In considering this last relationship of power, we can say that the resulting torque is a consequence of the collapse of the

current and/or voltage depending on the connection mode of the turbine to the grid. The rotation speed influences the fault frequency evolution, implicitly the relationship with faults signature.

The distribution of forces in accordance with the fault location is summarized in Table 1.

Owing to high pressure and friction exerted on the teeth, the weakest link in a wind generator is its gearbox. As turbine sizes increase, the design of a gearbox, which is able to handle the torque generated by longer and heavier blades becomes a problem. In a fault case, the turbine loading (force and

direction) is variable Fig. 3. Table 1 causes misalignment of the gearbox with the generator shafts and leads to failure.

So a broken tooth located at the gearbox, in addition to the defect frequency and duration it is characterized by a direction. Thus the magnitude and phase shift can inform us of the nature and position of the defect.

4 Experimental results and discussion

The advantage of symmetrical components vectors is the instantaneous calculation allowing an in time and online defections. So, during the experiment, two pins in the Digital Signal Controllers (DSPIC30F 3013) have been reserved to the analog to digital converter (ADC) conversion [20]. In order to improve the data treatment and accuracy, the signal synchronization is set to 100 μs.

In order to have all signal information during crossing time of the broken tooth, we set the synchronization time at 100 μs. This consideration allows more than 17,000 data points by convolution. Otherwise the signal information will be lost at high wind velocity.

The collected data are done after analog to digital conversion (ADC) provided in DSPIC microcontroller. Three arrays of the vectors wind velocity, current and voltage are reserved in the EPROM and cleaned after each blades convolution cycle.

For convenience, let us denote N_R, N_S and N_P as the number of teeth on the gears.

$N_{\mathbf{R}}$—Number of teeth in ring gear
$N_{\mathbf{S}}$—Number of teeth in sun (middle) gear
$N_{\mathbf{P}}$—Number of teeth in planet gears

The first constraint to a planetary gear to work properly is that all the teeth have the same tooth gap (7). This ensures an effective mechanical transmission without friction.

The second constraint is:

$$N_R = 2 \times N_P + N_S \tag{7}$$

The unbalance caused by a broken tooth Fig. 5 ("Appendix") at:

– Ring gear is repeated three times each blades convolution
– Planet gear is repeated 68/26 times each blades convolution
– Sun gear is repeated three (68/16) times each blades convolution

The frequency of occurrence of broken tooth default is quantified by the ratio between the number of teeth forming the ring gear and the concerned gear (8). Furthermore, the duration of the fault (9) depends on the rotation speed of the gear, in addition to the number of the total teeth, Fig. 5.

Vibration analysis is the dominant technique used for predictive maintenance programs. This technique uses the noise or vibration created by mechanical equipment to detect machine problems. The gear mesh frequency is the rate at which gear teeth engage together in the pitch point and it is equal to the number of teeth on the gear times the rpm of the gear.

The relation between the shaft rotation period and the tooth meshing period is,

$$F_R = F_B/k_R \; ; \; F_P = k_P F_B N_P/N_R \; ; \; F_S = k_S F_B N_S/N_R \tag{8}$$

$K_R = 3$, $k_P = 2$ and $k_S = 3$ are the contact gear number of, respectively, ring, planet and sun gear.

The time period elapsed between the moment when a tooth goes into meshing and the moment it goes out of meshing is called the tooth meshing period, T_R, T_P and T_S

$$T_R = 3/(F_B N_R); \; T_P = N_R/F_B N_P^2; \; T_S = 3N_R/F_B N_S^2 \tag{9}$$

where

F_B – Blade frequency
F_R – Ring fault frequency
F_P – Planet fault frequency
F_S – Sun fault frequency
T_R – Ring fault duration
T_P – Planet fault duration
T_S – Sun fault duration

These meshing forces generate vibrations [21] that are transmitted to other parts of the machine where they can be measured.

Several works dealing with this kind of defects use sound sensors inside the nacelle. Noise can be generated by various mechanisms. The most noise sources are vibrating surface, wind turbulence and blade, passing through air each of them produces its own vibration. Therefore, the waves propagating in different directions will interfere and complicate the diagnosis. The noise can be divided into two types, mechanical noise and aerodynamic noise. In this work, we propose to eliminate the aerodynamic effect and analyze the mechanical noise source only. Then instead of using the sound sensor, the measuring apparatus of wind turbine output power is used.

During the passage through the broken tooth, the effective force collapses to reach 2/3 of the force normally transmitted through the blades. In this short time, the average power generated by the wind decreases with the same proportion. This

Fig. 5 Fault sequences for each blade cycle
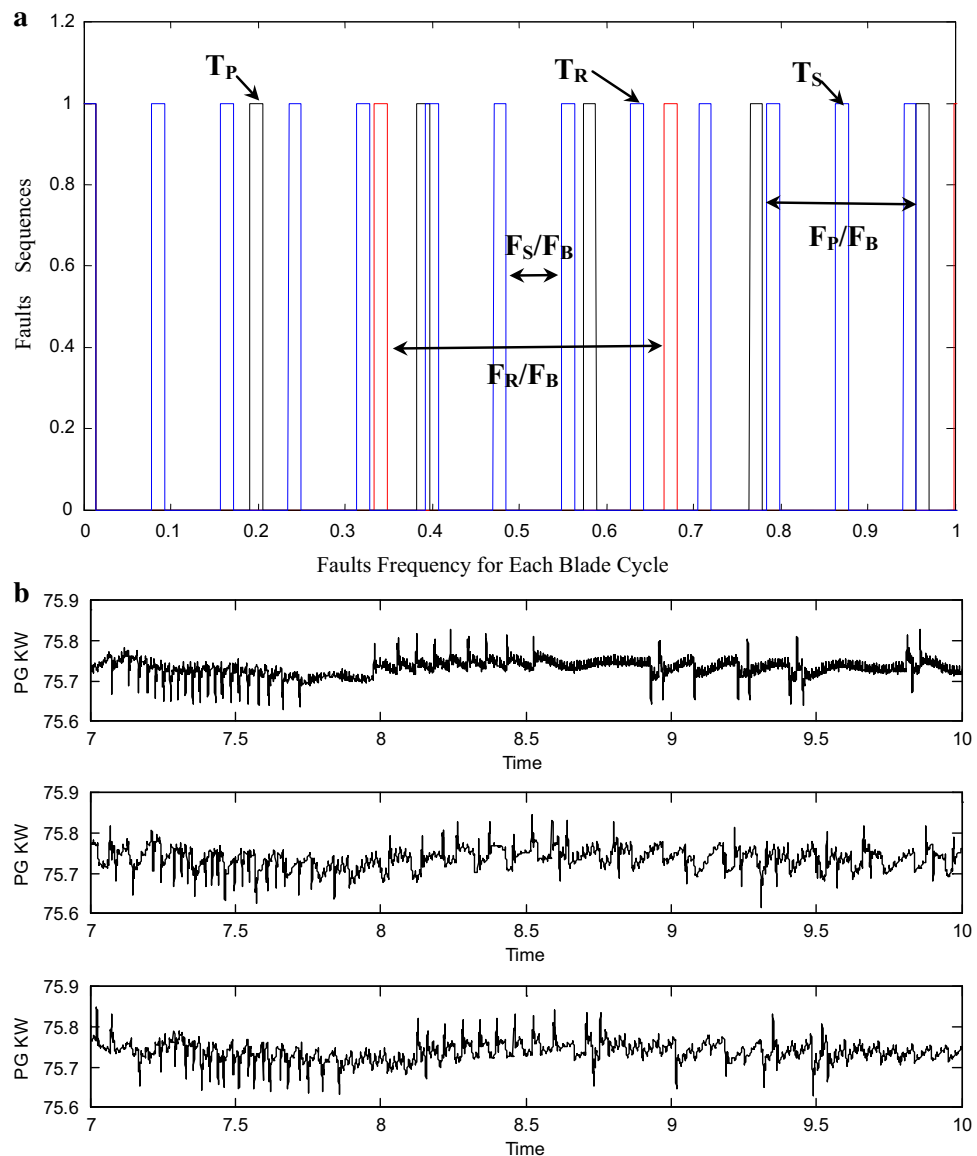
defect is cyclical, thanks to the spectral analysis, it appears as harmonic peaks [22]. Considering the difficulty of placing one or more sensors inside the gearbox, it is proposed to analyze the instantaneous active and reactive power waveform [23] Fig. 6a, b.

Why the power and not the current for example?

To detect a fault, we must make it visible. Then the use of two sinusoidal components in interaction (the power in the case of the voltage and current) allows the detection of the defect after a spectral analysis [24].

The current is mainly influenced by the wind power through the blade's torque (10), but the voltage is influenced mainly by the magnetic flux and the rotor speed (11). Both, rotor speed and torque depend on the teeth healthy condition

$$I = C/k\phi \tag{10}$$

$$V = k\phi\omega \tag{11}$$

So their growth amplifies the faults signature, to be much more significant.
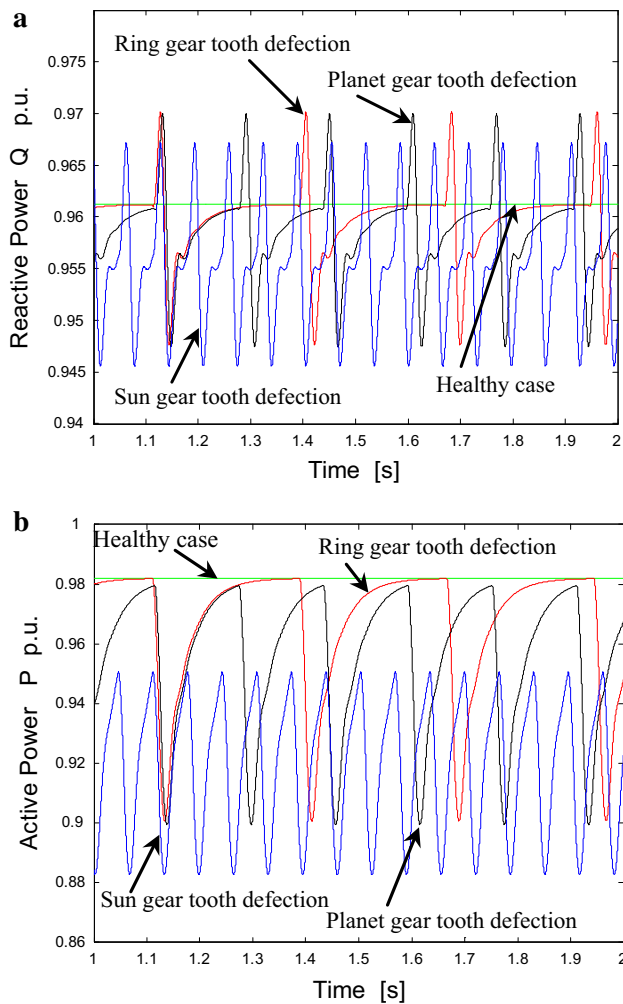
4.1 The instantaneous harmonics power load

The instantaneous power produced by the wind generator connected to the grid can be written as follows (12):

$$s_L(t) = \sqrt{3}.v_L(t).i_L(t) \tag{12}$$

Therefore, in its harmonics component form (13)

$$s_L = \sqrt{3}.\begin{bmatrix} v_{L1} & v_{L2} & . & v_{Lh} & . & v_{Ln} \end{bmatrix}.\begin{bmatrix} i_{L1} \\ i_{L2} \\ . \\ i_{Lh} \\ . \\ i_{Ln} \end{bmatrix} \tag{13}$$

Fig. 6 power ripple caused by a defection of the gearbox teeth

The developed form (14)

$$s_{\mathrm{L}} = \sqrt{3}.v_{\mathrm{L}1}.i_{\mathrm{L}1} + \sqrt{3}.v_{\mathrm{L}1}.\begin{bmatrix} i_{\mathrm{L}2} \\ i_{\mathrm{L}3} \\ . \\ i_{\mathrm{L}h} \\ . \\ i_{\mathrm{L}n} \end{bmatrix} + \sqrt{3}.i_{\mathrm{L}1}\begin{bmatrix} v_{\mathrm{L}2} \\ v_{\mathrm{L}3} \\ . \\ v_{\mathrm{L}h} \\ . \\ v_{\mathrm{L}n} \end{bmatrix}$$

$$+\sqrt{3}.\begin{bmatrix} v_{\mathrm{L}2} & v_{\mathrm{L}3} & . & v_{\mathrm{L}h} & . & v_{\mathrm{L}n} \end{bmatrix}.\begin{bmatrix} i_{\mathrm{L}2} \\ i_{\mathrm{L}3} \\ . \\ i_{\mathrm{L}h} \\ . \\ i_{\mathrm{L}n} \end{bmatrix} \qquad (14)$$

It should not be confused between the harmonic multiples of the mains frequency and the harmonics generated by the fault. Because in addition, these harmonics are lower than the

fundamental frequency one, but they are not integers (under-harmonics).

In general, the voltage waveform is very poor in harmonics [20], so, it can be assumed as only a fundamental component (15).

$$s_{\mathrm{L}}(t) \approx \sqrt{3}.v_{\mathrm{L}1}(t).i_{\mathrm{L}1}(t) + \sqrt{3}.v_{\mathrm{L}1}(t).\sum_{h=2}^{n} i_{\mathrm{L}h}(t) \qquad (15)$$

The interaction of harmonics currents with the power grid voltage generates also other types of power (16).

$$i_{\mathrm{L}h} = I_{\mathrm{L}h}\cos(h\omega t + \alpha_h)$$

$$S_{\mathrm{L},h}(t) = \sqrt{3}.v_{\mathrm{L}1}(t).\sum_{h=2}^{n} i_{\mathrm{L}h}(t)$$

$$S_{\mathrm{L},h}(t) = \sqrt{3}.V_{\mathrm{L}1}\sum_{h=2}^{n}[.I_{\mathrm{L}h}.\cos(\omega t).\cos(h\omega t + \alpha_h)]$$

$$S_{\mathrm{L},h}(t) = \sqrt{3}.V_{\mathrm{L}1}\sum_{h=2}^{n}[.I_{\mathrm{L}h}.\cos((h-1)\omega t + \alpha_h)]$$

$$+\sqrt{3}.V_{\mathrm{L}1}\sum_{h=2}^{n}[.I_{\mathrm{L}h}.\cos((h+1)\omega t + \alpha_h)] \qquad (16)$$

According to this expression (16), two new types of power can be extracted:

– Ripple active power

$$P_{\mathrm{L},h}(t) = \sqrt{3}.V_{\mathrm{L}1}\sum_{h=2}^{n} I_{\mathrm{L}h}.[\cos((h-1)\omega t) \\ + \cos((h+1)\omega t)].\cos(\alpha_h) \qquad (17)$$

– Ripple reactive power

$$Q_{\mathrm{L},h}(t) = -\sqrt{3}.V_{\mathrm{L}1}\sum_{h=2}^{n} I_{\mathrm{L}h}.[\sin((h-1)\omega t) \\ + \sin((h+1)\omega t)].\sin(\alpha_h) \qquad (18)$$

The symmetrical components allow instantaneous measurements of torques against an average measurement of torques by blade convolution. The effect on the instantaneous power is therefore easily evaluated and pointed out. So, the Discrete Fourier Transformation (DFT) is accurate, and its application for a discrete signal *y(nt)* is given by (19):

$$Y(k) = \sum_{n=0}^{N-1} y[nt]\,e^{-j\frac{2\pi}{N}nk} \qquad (19)$$

Fig. 7 Harmonics spectrum fault signature
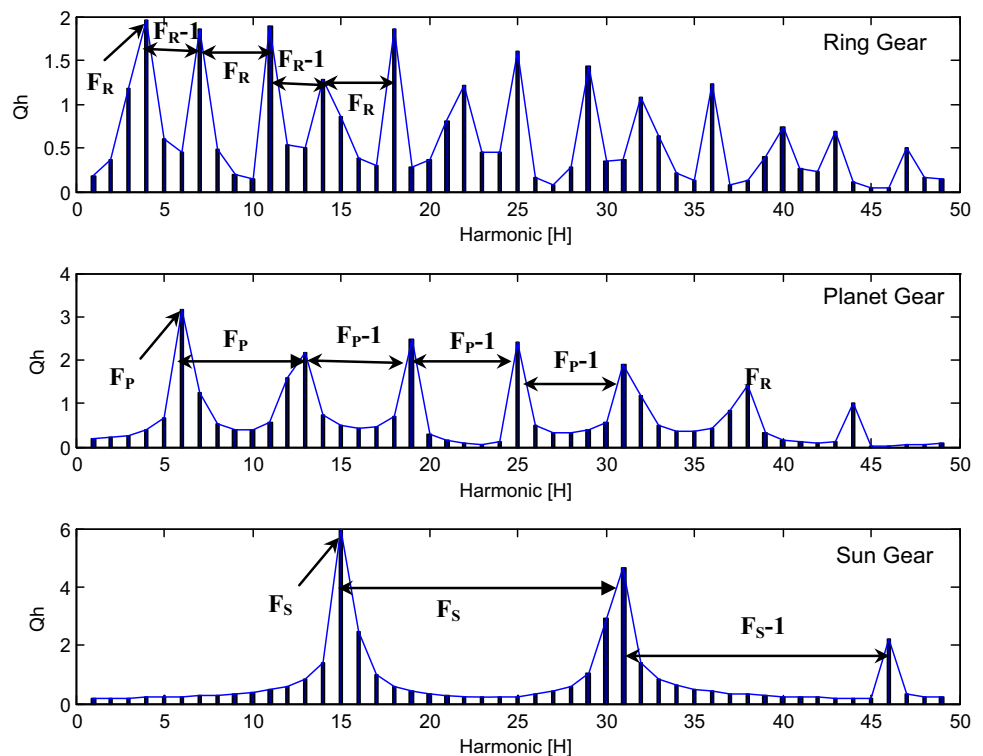
where $k = 0, 1, \ldots, N - 1$ and N is the samples number

$$Y = \begin{bmatrix} y(0)e^{-j\frac{2\pi}{N}0.0} & y(1)e^{-j\frac{2\pi}{N}1.0} & \ldots & y(N-1)e^{-j\frac{2\pi}{N}(N-1).0} \\ y(0)e^{-j\frac{2\pi}{N}1.1} & y(1)e^{-j\frac{2\pi}{N}1.1} & \ldots & y(N-1)e^{-j\frac{2\pi}{N}(N-1).1} \\ \vdots] & \ldots & \ldots & \vdots \\ y(0)e^{-j\frac{2\pi}{N}1.(N-1)} & y(1)e^{-j\frac{2\pi}{N}1.(N-1)} & \ldots & y(N-1)e^{-j\frac{2\pi}{N}(N-1).(N-1)} \end{bmatrix} \qquad (20)$$

To evaluate all the given values Y(k) DFT requires *NxN* operations and *NxN* number to be stored in the memory (20). Fortunately $e^{-j\frac{2\pi}{N}nk}$ is periodical and symmetrical the matrix Y can be divided in two simplified matrix odd and even (21), as follows:

$$Y(2n + 1) = Y(1) + Y(3) + \cdots + Y(N - 1)$$
$$Y(2n) = Y(0) + Y(2) + \cdots + Y(N - 2) \qquad (21)$$

This last formulation reduces the calculation number to $N/2$ operations. This improves the time calculation of the DFT algorithm and the required memory for harmonics components determination.

So at the time of the fault, we will have a center frequency surrounded by pairs of frequencies at the right and left with a same distance (17-18).

While the oscillations magnitudes of the instantaneous active power are greater than that of the reactive power, we believe that the analysis of defects by reactive power is better, because the fault occurs on the active power as shock

waves Fig. 6b. In the instantaneous reactive power the disturbances are closer to an oscillation Fig. 6a, so they can be characterized by a frequency in addition to their amplitude [25].

Indeed, the location of the broken tooth influences the torque distribution, which varies in the gearbox.

Knowing that the wind velocity is variable, the harmonics spectrum fault signature changes. This velocity permits the rotation of blades (22); in other words, blades' rotation frequency (23)

$$\omega_B = V_B / R_B \qquad (22)$$
$$F_B = \omega_B / 2\pi \qquad (23)$$

And applying the relation (9) for any wind velocity one can find that the faults signature keeps the same ratio between the fault frequency and F_B.

If $F_{Fault}/F_B = N_R/3$ The fault is located in the ring gear
$F_{Fault}/F_B = N_P^2/N_R$ The fault is located in the planet gear
$F_{Fault}/F_B = N_S^2/(3N_R)$ The fault is located in the sun gear

Unlike other defects that may affect the wind, the faults inside the gearbox are manifested by under-harmonics [26]. For a wind speed of 10 m/s the first center frequency is respectively $F_R = 3.6$ Hz; FP= 6.3 Hz and $F_S = 15.3$ Hz. So, the quantity between two successive harmonics rays can set the location of the fault in the gearbox [26,27] Fig. 7.

In the experience we have use sensors for wind velocity, output current and voltage. In the DSPIC program the wind velocity is used as time base for DFT. The ratio of the first significant under harmonic frequency is displayed by the LCD. The value of this ratio informs us about the gearbox healthy, and the location of the broken tooth if any. This information can be used as a warning alert sent by the supervisor program to the operator.

Failure signature [28] at the ring gear or at the sun gear is obvious because there is only one ring gear and one sun gear. But for the planet gear we need another parameter to define exactly which of the three planet gears is in default. Fortunately, the modeling by the symmetrical components method permits the measurement of the Zero sequence $F_{0,X}$ component that exerts pressure on the shaft, leading to an eccentricity opposite to the planet gear in fault Table 1.

Compared to the other results found in other papers where the turbine gearbox faults are detected as an overall fault inside the entire device, our proposal permits to define the location of a broken tooth inside the turbine gearbox.

5 Conclusion

Early detection of the fault allows the scheduling, thus reducing the economic loss. One of the most difficult elements to detect in the wind is the default in the gearbox, because of its inaccessibility. Modeling based on the symmetrical components method associated with the frequency domain technique permits an accurate sensor-less identification of the diagnosis inside the gearbox. In addition, an instantaneous evaluation is possible, because the relationship between the instantaneous power and fault location is pointed out. In fact, by the method of symmetrical components, the quantification of a useful force, antagonist force and those responsible of the shaft eccentricity are possible. Combining spectral analysis allows the separation of the defects signature in the gearbox from the other defections of the devices inside the nacelle.

Appendix

See Table 2.

Table 2 Parameters for 550 KW wind planetary gearbox (PG-B)

	Sun	Ring	Carrier	Planet
Mass (kg)	51	4	1.330	114
Moment of inertia	61.1	2.484	314.7	51.9
Number of teeth	16	68	–	26
Rotor diam. (mm)	202	980	–	329
Pitch diam. (mm)	224	952	–	364

References

1. Yang Yu, Yu Dejie, Cheng J (2007) A fault diagnosis approach for roller bearing based on IMF envelope spectrum and SVM. Measurement 40:943–950
2. Schlechtingen M, Santos IF (2011) Comparative analysis of neural network and regression based condition monitoring approaches for wind turbine fault detection. Mech Syst Signal Process 25(5):1849–18757
3. Zhi-Ling Y, Bin W, Xing-Hui D, Hao L (2012) Expert system of fault diagnosis for gear box in wind turbine. Syst Eng Proced 4:189–195
4. Barszcz T, Randall RB (2009) Application of spectral kurtosis for detection of a tooth crack in the planetary gear of a wind turbine. Mech Syst Signal Process 23:1352–1365
5. Chen F, Tang B, Chen R (2012) A novel fault diagnosis model for gearbox based on wavelet support vector machine with immune genetic algorithm. Measurement 46:220–232
6. Tang B, Liu W, Song T (2010) Wind turbine fault diagnosis based on Morlet wavelet transformation and Wigner-Ville distribution. Renew Energy 35:2862–2866
7. Lei Y, Zuo JM, He Z, Zi Y (2010) A multidimensional hybrid intelligent method for gear fault diagnosis. Expert Syst Appl 37:1419–1430
8. Schlechtingen M, Santos IF (2011) Comparative analysis of neural network and regression based condition monitoring approaches for wind turbine fault detection. Mech Syst Signal Process 25(5):1849–1875
9. Zhang Z; 3131 Seamans center, University of Iowa, Iowa city, IA, USA. Verma A, Kusiak A (2012) Fault analysis and condition monitoring of the wind turbine gearbox. IEEE Trans Energy Convers 27(2):526–535
10. Lu B, Li Y, Wu X, Yang Z (2009) A review of recent advances in wind turbine condition monitoring and fault diagnosis. IEEE Power Electron Mach Wind Appl 2009:1–7
11. Yang S, Computer Deptartment, ShanDong Institute of Bus and Technology. Yantai; Li W, Wang C (2008) The intelligent fault diagnosis of wind turbine gearbox based on artificial neural network. In: IEEE International Conference on Condition Monitoring and Diagnosis, 2008. CMD 2008. 21–24 April 2008, pp 1327–1330
12. Tang B, Liu W, Song T (2010) Wind turbine fault diagnosis based on Morlet wavelet transformation and Wigner-Ville distribution. Renew Energy 35(12):2862–2866
13. Yang W Renewable energy centre. Blyth UK, Tavner PJ, Crabtree CJ, Wilkinson M (2010) Cost-effective condition monitoring for wind turbines. IEEE Trans Ind Electron 57(1):263–271
14. Barszcz T, Randall RB (2009) Application of spectral kurtosis for detection of a tooth crack in the planetary gear of a wind turbine. Mech Syst Signal Process 23(4):1352–1365
15. Liu WY, Zhang WH, Han JG, Wang GF (2012) A new wind turbine fault diagnosis method based on the local mean decomposition. Renew Energy 48:411–415

16. Soua S, Van Lieshout P, Perera A, Gan TH, Bridge B (2013) Determination of the combined vibrational and acoustic emission signature of a wind turbine gearbox and generator shaft in service as a pre-requisite for effective condition monitoring. Renew Energy 51:175–181

17. Guo Y, Parker RG (2010) Dynamic modeling and analysis of a spur planetary gear involving tooth wedging and bearing clearance nonlinearity. Eur J Mech Sol 29(6):1022–1033

18. Florkowski M, Furgał J (2009) Modelling of winding failures identification using the frequency response analysis (FRA) method. Electr Power Syst Res 79(7):1069–1075

19. Morsi WG, El-Hawary ME (2011) On the application of wavelet transform for symmetrical components computations in the presence of stationary and non-stationary power quality disturbances. Electr Power Syst Res 81(7):1373–1380

20. Xuejun Z, Yu C (2005) The research of intelligent fault diagnosing methods based on FTA. Microcomput Inf 21(6):123–124

21. Saravanan N, Cholairajan S, Ramachandran KI (2009) Vibration-based fault diagnosis of spur bevel gear box using fuzzy technique. Expert Syst Appl 36:3119–3135

22. Li C, Liang M (2012) Time-frequency signal analysis for gearbox fault diagnosis using a generalized synchrosqueezing transform. Mech Syst Signal Process 26:205–217

23. Feng Z, Liang M, Zhang Y, Hou S (2012) Fault diagnosis for wind turbine planetary gearboxes via demodulation analysis based on ensemble empirical mode decomposition and energy separation. Renew Energy 47:112–126

24. Zhou X, Luo D (2012) Research of amplitude-frequency domain parameters analysis for condition detection and fault diagnosis. Res J Appl Sci Eng Technol 4(19):3787–3790

25. Wenyi L, Zhenfeng W, Jiguang H, Guangfeng W (2013) Wind turbine fault diagnosis method based on diagonal spectrum and clustering binary tree SVM. Renew Energy 50:1–66

26. Saravanan N, Kumar Siddabattuni VNS, Ramachandran KI (2008) Comparative study on classification of features by SVM and PSVM extracted using Morlet wavelet for fault diagnosis of spur bevel gear box. Expert Syst Appl 35:1351–1366

27. Hussain S, Gabbar HA (2011) A novel method for real time gear fault detection based on pulse shape analysis. Mech Syst Signal Process 25:1287–1298

28. Jiang Y, Tang B, Qin Y, Wenyi L (2011) Feature extraction method of wind turbine based on adaptive Morlet wavelet and SVD. Renew Energy 36:2146–2153